Contribution from the Departments of Chemistry, Iowa State University, Ames, Iowa 50011, and University of California, Davis, California 95616

$Y_{10}I_{13}C_2$: A Novel Compound with Chains of both Carbon-Centered and Empty Clusters

Susan M. Kauzlarich,[1a] Martin W. Payne,[1b] and John D. Corbett*[,1b]

Received December 18, 1989

The phase $Y_{10}I_{13}C_2$ is synthesized by the reaction at ~800 °C of powdered Y and YI_3 with impure Y_2O_3, the vital carbon component resulting from incomplete decomposition of the yttrium oxalate precursor. The phase has not been obtained from more conventional carbon sources. The identity of carbon as the interstitial is supported by these syntheses, microprobe analyses of $Y_{10}I_{13}C_2$ vs $Y_6I_7C_2$, and both the occupancy and the dimensions of the yttrium cavity in which carbon occurs. The phase occurs in space group $C2/m$, $Z = 2$; $a = 21.317$ (6) Å; $b = 3.957$ (1) Å; $c = 19.899$ (5) Å; $\beta = 97.40$ (2)°; $R/R_w = 3.3\%/3.9\%$ for 838 independent reflections with $2\theta \leq 50°$ (Mo Kα). The compound consists of centered $Y_6I_{12}C$- and empty Y_6I_8-type clusters condensed by edge sharing into commensurate double and single chains, respectively. The chains are further cross-linked by additional iodine atoms. The two chain types are very similar to those known individually in the phases $Y_6I_7C_2$ and Y_4Cl_6 and are presumably metallic and semiconducting, respectively. The Y_4I_6 chain is the first iodide example of condensed Y_6X_8-type clusters. This feature appears to be stabilized in this structure by a sterically less demanding means of bridging these chains between sheets of a $Y_6I_7C_2$-like arrangement.

Introduction

An explosion of novel phases containing octahedral metal clusters and condensed clusters has taken place in recent years among the reduced halides of the transition elements from groups 3 and 4. This large family of new compounds arises because of the additional stability and versatility conferred to relatively electron-poor clusters through inclusion of an interstitial element within each cluster. The diversity of elements that may play the role of the interstitial is remarkable indeed, particularly in the iodides. Isolated R_6X_{12}-type octahedral clusters constructed of rare-earth elements (R) are now known with encapsulated B-N,[2,3] C_2,[4-6] Mn-Cu,[7,8] Re, Au,[8] and all of the platinum metals.[8,9] Similar centered clusters condensed at trans edges into infinite single chains are also found in Sc_5Cl_8(C or N),[10] in Sc_4Cl_6(B or N),[2] in Y_4I_5C,[11] and, as double chains, in $Sc_7Cl_{10}C_2$,[12] $Y_6I_7C_2$,[11] and some gadolinium analogues.[5]

Not all rare-earth-metal cluster chains need contain interstitial atoms. True binary phases of this sort are encountered in Y_4Cl_6 and Y_4Br_6,[13] both of which have the parent Gd_4Cl_6 structure, and in Sc_7Cl_{10}.[12,14] However, the construction of these chains is clearly distinct from that of the centered examples. The empty chains can all be viewed as products of the condensation of R_6X_8-type clusters in which halide X caps the (exposed) triangular faces rather than the edges of the metal octahedra. Yttrium iodides evidently do not form these or any other binary reduced phases, the YI_3-Y interaction apparently being limited to the solution of ~12 mol % metal in molten YI_3 at its melting point.[15]

Attempts to introduce oxygen interstitials into any type of cluster halide have been notably unproductive, the exception being the solid solutions known in the layered $ZrXO_y$ phases, X = Cl or Br, $0 \leq y \leq \sim 0.40$. Oxygen in these occupies tetrahedral interstices between the double zirconium layers.[16] In contrast, the ubiquity of ROX contaminants (PbFCl structure) originating from the nearly inevitable oxygen impurities has been a feature of all studies of rare-earth-metal chloride and many iodide systems. Notwithstanding, an exploration of cluster phases in the Y-O-I system was prompted by the idea that the alternate ROI phases are more nearly layered than three-dimensional[17] and the observation that states in the metal-based conduction band in Y_4I_5C and $Y_6I_7C_2$[11] remain bonding for some interval above E_F. In fact, impurities in our source of the potential interstitial, Y_2O_3, turned out to give us a new chemistry by producing the carbide, $Y_{10}I_{13}C_2$, a phase that cannot be obtained from other more conventional carbon sources. Considerable synthetic effort, together with guidance from structural and microprobe data, was needed to reproduce the synthesis by design.

Experimental Section

The metal initially employed had been produced and distilled within Ames Laboratory and had the following typical impurities (atom ppm): O, 250; N, 13; H, 616; C, 104; F, 131; Fe, 27; W, 20; Gd, 8.1; La, 5.3; Tb, 4.0; Pr, 8; Ce, 2.8; other lanthanides, <1. Later work used a vacuum-sublimed Johnson Matthey/AESAR product. Metal from the first source was cold-rolled into strips about 4 × 10 × 0.04 cm, cleaned with minimal exposure to air, and cut into narrow strips. Dendritic pieces from the second metal source were used directly or converted to powder. The Y_2O_3 also obtained from Ames Laboratory was 99.999% on a metals basis. Most procedures were carried out as described previously: the preparation and sublimation of YI_3, the preparation of powdered Y, reactions in sealed Nb containers, Guinier powder pattern measurements, and lattice constant refinement techniques.[7,11,12]

Syntheses. The first reactions of Y, YI_3, and Y_2O_3 were loaded for the compositions Y_4I_5O, $Y_6I_7O_2$, and $Y_7I_{10}O_2$ based on the stoichiometries of known carbide phases and were reacted at 800–900 °C. A new phase in the form of fine black needles was obtained sporadically in low yields and was subsequently shown to be $Y_{10}I_{13}C_2$. Powder patterns calculated on the basis of the structure reproduced the experimental patterns completely except for contributions from YI_3 and YOI (PbFCl structure). The presence of carbon in what was first thought to be an oxide was suggested by structural studies (below) and was later established by microprobe analyses of several crystals and by more direct syntheses. Microprobe analyses of several of the new crystals were obtained on an automated Cameca SX-50 electron microprobe capable of quantitative analysis for all elements heavier than boron. Crystals of both $Y_6I_7C_2$ and $Y_{10}I_{13}C_2$ were pressed into indium but not polished. A rapid transfer of the holder in air into the instrument was necessary, which made oxygen and iodine analyses meaningless. (The new compound clearly was the more reactive.) Analyses were made on what appeared to be the flattest surfaces, and the Y:C ratio in $Y_6I_7C_2$ was used as a standard. Data for several crystals with total recoveries of Y, I, C, and O close to 100% gave an average Y:C ratio of about 10:2.7 for the new phase.

(1) (a) University of California. (b) Iowa State University.
(2) Hwu, S.-J.; Corbett, J. D. *J. Solid State Chem.* **1986**, *64*, 331.
(3) Dudis, D. S.; Corbett, J. D.; Hwu, S.-J. *Inorg. Chem.* **1986**, *25*, 3434.
(4) Warkentin, E.; Masse, R.; Simon, A. *Z. Anorg. Allg. Chem.* **1982**, *491*, 323.
(5) Simon, A. *J. Solid State Chem.* **1985**, *57*, 2.
(6) Dudis, D. S.; Corbett, J. D. *Inorg. Chem.* **1987**, *26*, 1933.
(7) Hughbanks, T.; Corbett, J. D. *Inorg. Chem.* **1988**, *27*, 2022.
(8) Payne, M.; Corbett, J. D. *Inorg. Chem.* **1990**, *29*, 2246.
(9) Hughbanks, T.; Corbett, J. D. *Inorg. Chem.* **1989**, *28*, 631.
(10) Hwu, S.-J.; Dudis, D. S.; Corbett, J. D. *Inorg. Chem.* **1987**, *26*, 469.
(11) Kauzlarich, S. M.; Hughbanks, T.; Corbett, J. D.; Klavins, P.; Shelton, R. N. *Inorg. Chem.* **1988**, *27*, 1791.
(12) Hwu, S.-J.; Corbett, J. D.; Poeppelmeier, K. R. *J. Solid State Chem.* **1985**, *57*, 43.
(13) Mattausch, H. J.; Hendricks, J. B.; Eger, R.; Corbett, J. D.; Simon, A. *Inorg. Chem.* **1980**, *19*, 2128.
(14) Poeppelmeier, K. R.; Corbett, J. D. *Inorg. Chem.* **1977**, *16*, 1107.
(15) Corbett, J. D.; Pollard, D. L.; Mee, J. E. *Inorg. Chem.* **1966**, *5*, 761.
(16) Seaverson, L. M.; Corbett, J. D. *Inorg. Chem.* **1983**, *22*, 3202.
(17) Hulliger, F. *Structural Chemistry of Layer-Type Phases*; Lévy, F., Ed.; D. Reidel Publishing Co.: Dordrecht, Holland, 1976; p 259.

0020-1669/90/1329-3777$02.50/0

Table I. Data Collection and Refinement Parameters for $Y_{10}I_{13}C_2$

space group, Z	$C2/m$ (No. 12), 2	fw	2562.84
cell dimens[a]		temp, °C	20
a, Å	21.307 (2)	μ(Mo Kα), cm^{-1}	293.2
b, Å	3.953 (1)	abs cor range	1.181–0.943
c, Å	19.899 (2)	R,[b] %	3.3
β, deg	97.40 (1)	R_w,[c] %	3.9
V, Å^3	1662.1 (1)		

[a] Cell parameters refined from Guinier pattern data with the aid of an internal Si standard are generally more accurate: a = 21.317 (6), b = 3.957 (1), c = 19.899 (5) Å; β = 97.40 (2)° (λ = 1.540 56 Å). [b] $R = \sum||F_o| - |F_c||/\sum|F_o|$. [c] $R_w = [\sum w(|F_o| - |F_c|)^2/\sum w(F_o)^2]^{1/2}$; $w = 1/\sigma(F)^{-2}$.

Combustion analysis of the original Y_2O_3 (Galbraith Laboratories) gave 0.12 wt % C. Another source of Y_2O_3 (CERAC) as well as $Y_2(C_2O_4)_3 \cdot nH_2O$ (dried at 120 °C), $Y_2(CO_3)_3 \cdot 3H_2O$, YC_2 (Aldrich), graphite (CERAC), and charcoal did not give recognizable amounts of $Y_{10}I_{13}C_2$. On the other hand, the last three and the oxalate produced the customary $Y_6I_7C_2$ in relatively good yields. Reactions of Y and YI_3 alone under comparable conditions yield only occasional traces of known iodide carbides[11] although one example did yield ~10% $Y_{10}I_{13}C_2$, which corresponds to 0.1 wt % carbon contamination.

In order to study the reactivity of incompletely ignited Y_2O_3, $Y_2(C_2O_4)_3 \cdot 9H_2O$ contained in a fused silica boat was decomposed in a tube furnace with somewhat restricted air flow and under various time and temperature conditions to establish empirically the relative extents of reaction. Samples that were ~50, 77, 86, and 96% decomposed based on weight loss were then prepared with the aid of these results. For reference, 75% of the theoretical weight loss corresponds to removal of all of the water plus 56% decomposition of the oxalate to Y_2O_3.

The presence of EDTA is known to affect the character of the oxalate formed,[18] and the nitrogen might also be involved as an interstitial. Therefore, the production process was also replicated, yttrium(III) being eluted from a Dowex column with a known amount of $(NH_4)_3$(HEDTA) and reacted as before with oxalate. Decomposed samples gave finer powders than without EDTA. The colors in both series were typically white, tan, gray, and off-white, respectively.

Crystallography. Several needlelike crystals from the reactions described above were examined by Weissenberg photographs, which indicated a C-centered monoclinic cell that lacked additional absences. The space group $C2/m$ was then tentatively selected on the basis of known examples.[10-13] Two of the better diffracting crystals were used for data collection on a Syntex $P2_1$ and, later, on a CAD-4 four-circle diffractometer. Although these diffracted copper radiation very well, the intensities obtained on the diffractometers with Mo Kα X-rays were generally quite low. (Mo Kα falls on the yttrium absorption edge.) Initial attempts to solve the structure with the first data set and MULTAN were not successful and neither were methods similar to those applied with $Sc_6I_{11}C_2$.[6] Likewise, a structural solution could not be found with second data set.

A third data set was then collected from a larger crystal that had been obtained later from a pseudobinary Y–YI_3 reaction noted above in which carbon evidently had been present as an impurity. In this case, 1287 independent observed reflections were available to 2θ = 55°, and the structure was solved by direct methods (SHELXS-86[19]), the output providing what turned out to be the correct positions for all 12 heavy atoms as well as for the interstitial, which at the time was presumed to be oxygen.[20] Routine absorption correction (four ψ scans, averaged) and refinement of the heavy atoms anisotropically yielded residuals R/R_w of 5.9%/7.0% at convergence. Allowing the multiplicities of all but one of the heavy atoms to vary was without effect. Of particular importances was the fact that no peak >1 e/Å^3 was apparent in either Fourier or different Fourier maps at 0, 0, 0, the center of metal octahedra that define a single chain in the structure. The fact that no further refinement was possible appeared to reflect some intrinsic problems in the data set, probably owing to movement of the crystal during data collection.

The structural model was then applied to the earlier CAD-4 data set after correction for absorption by an empirical method[21] (Table I). An interstitial in the double chain was clearly indicated, and with oxygen at this site the refinement converged at R/R_w = 3.4%/3.9%. The isotropic thermal parameter for oxygen was relatively large at this point. In view of the possible influence of the rather noisy ΔF map (below), the B was fixed at 2.2 Å^2, giving 0.75 (4) for the occupancy, effectively that of a carbon atom. The two largest peaks in the final difference Fourier map, 3.0 and 2.0 e/Å^3, lacked a logical explanation and may have originated with the absorption correction method employed with such strongly absorbing material (μ = 293.2 cm^{-1}). This interstitial was changed to carbon once synthetic and microprobe studies supported this assignment. The C atom refined to an occupancy of 0.92 (4), B = 0.8 (5) Å^2, at R/R_w = 3.3%/3.9% with all other variables free.

In order to confirm that the foregoing residual peaks were artifacts, the original Syntex data set was also refined after a numerical absorption correction had been applied (two ψ scans[22]). Although a smaller number of independent reflections were available, the solution gave a satisfactory result (R/R_w = 4.2%/4.2% with oxygen at 0.69 (5) occupancy, B = 2.2 Å^2) (Table I). More important, the highest peaks in the ΔF map, 1.1 and 0.9 e/Å^3, were near heavy atoms. Positional and thermal parameters obtained for the last two refinements had similar standard deviations, and the values of the atom coordinates in the two parameter sets differed by no more than 2σ. In view of these structures, the structure as determined with the first (CAD-4) data set is assumed to be complete, and its results are used in subsequent tabulation, discussion, and illustration of the structure.

A most interesting aspect of the two better refinements was that *both* data sets exhibited larger than average values of B_{11} for I4 and I7 as well as of B_{33} for I6, indicating that these probably reflect a real property of the structure. A torsional motion or disorder along the Y_4I_6 chain (below) is consistent with these effects.

Results and Discussion

The initial structural refinements assumed that the obvious interstitial present in one chain in the structure (below) was oxygen, since Y_2O_3 had been added for that purpose. However, the result was somewhat troubling; the ellipsoid for the oxygen interstitial was large, 4.9 (7) Å^2 vs a 1.22 Å^2 average for the remaining atoms, and its occupancy refined to close to that for a carbon atom when B was fixed at 2.2 Å^2. Moreover, the Y–"O" distances in the "$Y_6I_7O_2$" chain (below) were very similar to the corresponding values known in $Y_6I_7C_2$.[11] In addition, low yields of the new phase were obtained *only* when a local sample of Y_2O_3 was used as an interstitial source.

On the basis of the unusual synthetic and structural results, we postulated that the seemingly exclusive synthesis of what appeared to be a carbide originated with a carbon impurity in Y_2O_3 and that this derived from incomplete ignition of the oxalate. Combustion analysis of our sample gave the equivalent of 2.3 atom % C in Y_2O_3, and a semiquantitative microprobe analysis of some $Y_{10}I_{13}C_2$ crystals indicated the compound contained an appropriate amount of carbon. However, attempts to prepare the new phase from a wide variety of both customary and unusual sources of carbon (see Experimental Section) did not yield $Y_{10}I_{13}C_2$, only the previously known $Y_6I_7C_2$.

Purposely contaminated Y_2O_3 samples did afford $Y_{10}I_{13}C_2$ when used in Y:YI_3:Y_2O_3(C) proportions of ~5.5:5:1 and run at 800 °C for 1 week. The best reactions in this region were achieved with "Y_2O_3" that showed 85–95% of the theoretical weight loss on ignition. The low yields (≤20%) arose largely because the accompanying oxygen diverts much of the YI_3 to YOI. An excess of either Y or Y_2O_3(C) favors $Y_6I_7C_2$, and higher temperatures give the same result. Very seldom are both carbides obtained in appreciable amounts from the same reaction, $Y_{10}I_{13}C_2$ characteristically appearing as the smaller and finer black needles, often in clumps. Although gaseous CI_x species are believed to be involved in carbon transport and the ready formation of iodides like $Y_6I_7C_2$, the correct proportions of Y, YI_3, and C do not yield $Y_{10}I_{13}C_2$, and CO–CO_2 equilibria in these quasi-oxalate systems may be involved in carbon transport.[23] The presence of EDTA prior to the oxalate precipitation and decomposition has no effect on the synthesis, so nitrogen is not a significant interstitial component. The question of interstitial hydrogen was raised by one

(18) Burkholder, H. R. Private communication, 1989.
(19) Sheldrick, G. M. SHELXS-86. Institut für Anorganische Chemie, Universität Göttingen, FRG.
(20) Neutral-atom scattering factors and both parts of the anomalous scattering corrections were taken from: *International Tables for X-Ray Crystallography*; Kynoch Press: Birmingham, England, 1974; Vol. IV.
(21) DIFABS: Walker, N.; Stuart, D. *Acta Crystallogr.* **1983**, *A39*, 158.
(22) Karcher, B. A.; Jacobson, R. A. Unpublished program, Iowa State University, 1981.
(23) Schäfer, H. *Chemical Transport Reactions*; Academic Press: New York, 1964; pp 40, 124.

Table II. Positional Parameters and Their Estimated Standard Deviations for $Y_{10}I_{13}C_2$

atom	x	y	z	B_{iso}, Å^2
I1	0.11216 (9)	0.0	0.38034 (9)	1.09 (4)
I2	0.000	0.5	0.500	1.29 (6)
I3	0.21754 (9)	0.5	0.2678 (1)	1.29 (4)
I4	0.3430 (1)	0.0	0.1629 (1)	1.86 (4)
I5	0.42541 (9)	0.5	0.3299 (1)	1.18 (4)
I6	0.17108 (9)	0.0	0.0448 (1)	1.80 (4)
I7	0.0448 (1)	0.0	0.1822 (1)	1.68 (4)
Y1	0.0589 (1)	0.5	0.0614 (1)	1.31 (6)
Y2	0.2224 (1)	0.5	0.4317 (1)	0.82 (6)
Y3	0.1214 (1)	0.0	0.5306 (1)	0.87 (6)
Y4	0.4204 (1)	0.5	0.0870 (1)	0.43 (6)
Y5	0.3163 (1)	0.0	0.3278 (1)	1.05 (6)
C[b]	0.305 (1)	0.0	0.446 (1)	0.8 (5)

[a] Space group $C2/m$. [b] Occupancy = 0.92 (4).

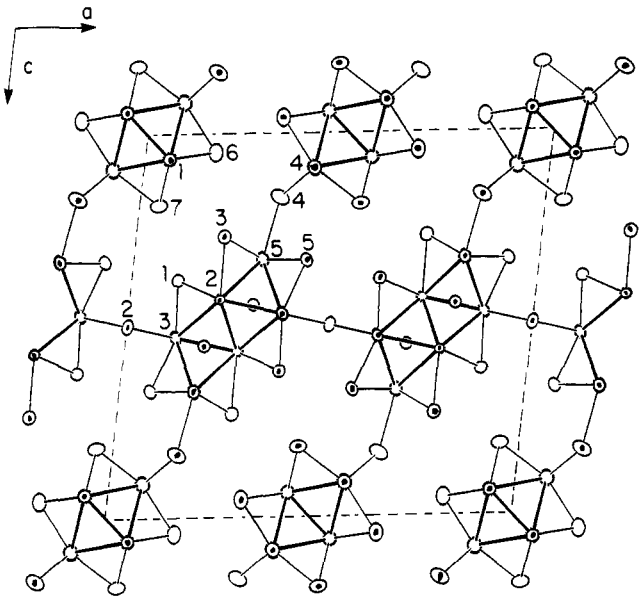

Figure 1. [010] projection of the structure of $Y_{10}I_{13}C_2$ with atom numbering. The yttrium and carbon atoms and the Y–Y cluster edges are emphasized. All atoms lie at $y = 0$ or $y = {}^1/_2$, with the latter dotted for clarity. (All figures employ 90% probability thermal ellipsoids.)

reviewer. This would have to result from hydrolysis accompanying dehydration of the oxalate and to be retained on decomposition at 800 °C or higher. Although the absence or presence of hydrogen cannot be ascertained, its necessity for stability of the new phase seems unlikely for several reasons: substantial hydride dissociation would probably occur at 800 °C, hydrogen readily passing through the Nb container at this temperature; no product was obtained with a charcoal source; the formation of hydride in each cluster in a semiconducting Y_4I_6 chain (there is no room in $Y_6I_7C_2$) would be expected to lead to recognizable distortions.

The Structure. Positional parameters for the $Y_{10}I_{13}C_2$ structure are listed in Table II, while important distances and angles therein are given in Table III. Anisotropic displacement parameters and structure factor data are contained in the supplementary material.

Figure 1 is projection of the structure down the short (3.97 Å) b (and needle) axis that also gives the labeling of the atoms. Yttrium and carbon atoms have the heavier outlines, and the metal atoms are interconnected by heavier lines. All atoms lie in mirror planes at $y = 0$ or $y = {}^1/_2$, the latter being designated in the figure by a dot on the atom. This construction generates infinite chains of nominal metal octahedra that share trans edges and have either exposed *faces* or *edges* capped by iodine. Single chains of condensed octahedra in a nominal Y_4I_6 face-capped unit lie along $0, y, 0$ and ${}^1/_2, y, 0$, while doubly condensed edge-bridged chains of metal octahedra that may be approximated as $Y_6I_7C_2$ are centered about ${}^1/_4, y, {}^1/_2$ and ${}^3/_4, y, {}^1/_2$. The slightly tilted view in Figure 2 shows these more clearly. The two chain types are

Table III. Distances[a] (Å) and Angles (deg) for $Y_{10}I_{13}C_2$

Distances			
	Y_4I_6		
Y1–Y1	3.269 (4)	I4–Y4 (×2)	3.088 (3)
Y1–Y4 (×2)	3.639 (4)	I6–Y1 (×2)	3.151 (3)
Y1–Y4 (×2)	3.627 (4)	I6–Y4	3.060 (3)
		I7–Y1 (×2)	3.154 (3)
		I7–Y4	3.053 (3)
	$Y_6I_7C_2$		
Y2–Y2 (×2)	3.442 (3)	I1–Y2 (×2)	3.138 (2)
Y2–Y3 (×2)	3.672 (3)	I1–Y3	2.968 (3)
Y2–Y3	3.314 (4)	I2–Y3 (×4)	3.249 (2)
Y2–Y5 (×2)	3.637 (3)	I2–Y2	3.249 (3)
Y3–Y5 (×2)	3.555 (3)	I3–Y5 (2)	3.019 (2)
Y2–C (×2)	2.64 (2)	I4–Y5	3.399 (4)
Y2–C	2.57 (3)	I5–Y3	3.067 (3)
Y3–2C (×2)	2.52 (2)	I5–Y5 (×2)	3.045 (3)
Y5–C	2.40 (3)		
I1–I2 (×2)	4.090 (2)[b]	I3–I4 (×2)	4.100 (3)
I1–I3 (×2)	3.908 (3)	I4–I5 (×2)	4.064 (2)
I1–I5	3.979 (2)[c]	I4–I6	4.087 (3)[c]
I1–I7	4.017 (3)[c]	I5–I7	4.125 (3)[c]
I2–I5 (×4)	4.061 (2)	I6–I7	4.073 (3)
Angles			
	Y_4I_6		
Y1–Y1–Y4	63.07 (7)	Y1–I6–Y4	71.44 (7)
Y4–Y1–Y4	65.76 (6)	Y1–I7–Y4	71.77 (7)
Y4–Y1–Y4	66.01 (6)	Y4–Y4–Y5	129.58 (7)
	$Y_6I_7C_2$		
Y2–Y5–Y2	65.80 (6)	Y2–I3–Y5	70.84 (7)
Y2–Y5–Y3	54.80 (6)	Y3–I5–Y5	71.14 (7)
Y3–Y5–Y3	67.52 (6)	C–Y2–C	96.8 (6)
Y2–I1–Y3	73.89 (7)	C–Y3–C	103.2 (6)
Y3–I2–I3	74.91 (4)		

[a] All atoms also have two like neighbors at $\pm b$, 3.957 (1) Å. [b] All nonbonding I–I distances ≤ 4.125. [c] Interchain I–I distances.

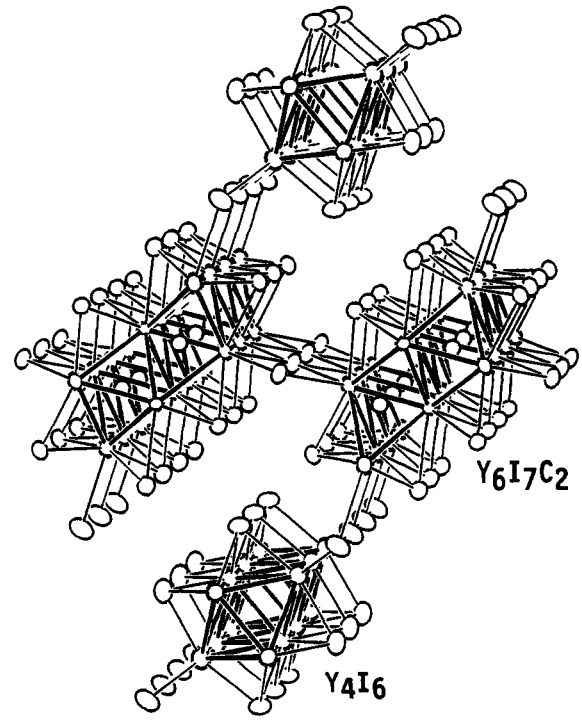

Figure 2. An off-[010] view of the $Y_{10}I_{13}C_2$ showing short portions of the infinite single (Y_4I_6, top, bottom) and double ($Y_6I_7C_2$, left, right) cluster chains and the intercluster iodine bridging.

interconnected through bridging iodine atoms I2 and I4 that bond in characteristic ways between yttrium vertices.

The two types of chains are very reminiscent of those known individually in the phases Y_4Cl_6[13] and $Y_6I_7C_2$,[11] respectively, when

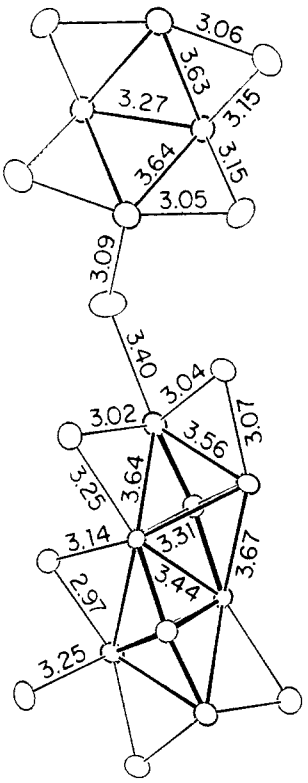

Figure 3. Projections of the two chains in $Y_{10}I_{13}C_2$ showing important Y–Y and Y–I distances.

the Y–I distances to bridging I4 are considered (Figure 3). Referring to Figure 1 for atom identifications, the I4 atom is bonded relatively tightly (3.09 Å) to pairs of Y4 vertices on the single cluster chain, while the I4–I5 distance in the double chain is appreciably longer, 3.40 Å, doubtlessly because of the close contacts I4 makes with I3 and I5 atoms on approaching the somewhat recessed Y5 vertex. Thus, the single chain can be readily described as $(Y4)_2(Y1)_{4/2}(I6,7)^i_{8/2}(I4)^a_{4/2} = Y_4I_6$ (i = inner, a = outer). The other bridging atom I2 is shared only between double chains. This portion cannot be described so easily, but the independent unit is $(Y2,3,5)_x(I1,3,5)^i_x(C)$, which, with a multiplicity x of $1 + {}^2/_2$ for each unit and ${}^1/_2 + {}^2/_2$ for the bridging $I2^{i-i}$, gives a total of $Y_6I_7C_2$. This ready simplification allows us to consider each chain type separately.

The Y_4I_6 Chain. This chain is remarkably similar to that long known in Gd_4Cl_6[24] and more recently defined in better detail in the isostructural Y_4Cl_6.[13] This structure is also known from powder data to occur for Y_4Br_6 as well as Tb_4Cl_6 etc.,[25] but the chains have not been seen before in an iodide. This circumstance probably arises because of the difficulty of interconnecting the chains in the same way by iodine atoms bridging between vertices Y1 and Y4. In the Gd_4Cl_6 structure, the shared metal atoms in the waist are also bonded to an inner halide in another chain and vice versa, a bonding interaction that would be considerably lessened by the larger contact radii of the four iodines that now surround Y1. In the present structure, Y1 is 4.97 Å from I3 (Figure 1), while I1–I7 and I4–I6 distances across the same gap are 4.02 and 4.09 Å, respectively, typical van der Waals diameters.

In addition, the interchain bridgings at the vertex atoms of the nominal metal octahedra in the two structures containing Y_4X_6 chains are really different. Three-coordinate I4 atoms bridge pairs of metal vertices in the Y_4I_6 chain and are terminal to a single more distant vertex in the double chain (Figures 1 and 2). An interchain bridging mode not seen elsewhere is present in Y_4Cl_6 (and Y_4Br_6). Here *two* rows of three-coordinate halogen atoms with the same connectivity link vertices in like chains in a mutually complementary manner, being alternatively bonded to two vertices in one chain and one in an adjoining chain that has been displaced by $b/2$. The contacts along and between these double rows of Cl^a atoms are the shortest in the structure, and two rather than three iodine atoms at each metal vertex are clearly dictated by halogen size.

The Y_4I_6 chains otherwise differ from those in Y_4Cl_6 in only a few respects. Not surprisingly, the chain repeat has increased to accommodate the larger non-metal, but only by 0.13 Å. Two independent Y–Y distances in the metal chain are the same as in the chloride, 3.27 Å (shared edge) and 3.64 Å, while the third, 3.63 Å, is a little shorter than 3.69 Å in the chloride, probably because chlorine on that metal face is also involved in the interchain bridging described above.

Structures that contain the R_4X_6 chains as well as those for Sc_7Cl_{10}[17] and ZrCl[26] have the distinctive feature that all consist of condensed octahedra *face-capped* by halide (M_6X_8 type); substantially all other halide examples are based on edge-bridged clusters (M_6X_{12}). All M_6X_{12} clusters involving transition metals from groups 3 and 4 apparently also bind an intestinal atom Z, and it has been argued that the M_6X_8Z analogues are not found because these would place face-capped X and Z too close to each other[12] (except perhaps for Z = H). (Presumably there are also electronic factors.) The emptiness of the Y_4I_6 chain in the present structure fits this classification. The overall similarity of the empty Y_4I_6 chain in $Y_{10}I_{13}C_2$ to that in the simpler Y_4Cl_6 encourages us to conclude that we are dealing with the electronic counterpart of the chloride in this more complex iodide. Resistivity,[27] UPS,[28] and theoretical[29] evidence indicate that Gd_4Cl_6 has a filled valence band (i.e., a well-split d band) and is a semiconductor ($E_g \sim 0.8$ eV), and the same is expected for the Y_4I_6 component in this structure.

The $Y_6I_7C_2$ Chain. This double-chain portion of the $Y_{10}I_{13}C_2$ structure is remarkably like that recently described in $Y_6I_7C_2$.[11] In fact, the horizontal section across the midpoint of Figure 1 that contains the $Y_6I_6C_2$ units bridged by four-coordinate I2 is virtually the unit cell of the $Y_6I_7C_2$. The interconnections more or less along $\vec{c}$ in the earlier example are pairs of even longer (3.59 Å) bridges formed by the equivalent of an inner I5 atom in one chain bonding to Y5 in an identical adjoining sheet, and vice versa. Distances within and between the two examples of double carbide chains are very similar except for a general lengthening of the chain repeat along $\vec{b}$ by 0.048 Å in the present structure. Otherwise, equivalent Y–Y and Y–I distances are within ±0.03 Å in the two phases except for those about Y5 and I2 associated with the different modes of interchain bonding (above). As seen in $Y_6I_7C_2$ and $Sc_7Cl_{10}C_2$, the carbon atoms are displaced toward the presumably more positive metal atoms that have fewer metal and more iodine neighbors, Y3 and Y5. Although the average Y–C distance is 0.02 Å larger here than in $Y_6I_7C_2$, this is probably not significant in view of the errors in the structure parameters (Table II). The chains are likely to be metallic, as in $Y_6I_7C_2$.[11]

The average Y–C distance of 2.55 Å in $Y_{10}I_{13}C_2$ was one of the earliest indications that this phase was not an oxide. Were this to be the case, these distances would be expected to be about 0.05 Å smaller on the basis of numerous regularities we have found for effective interstitial sizes in zirconium clusters.[30] The fact that an oxide does not form in spite of expectations of increased Y–Y bonding from the additional electrons (cf. Introduction) must be attributed to a greater stability of an alternate phase (YOI), a factor that naturally that does not enter into the calculations.

The structure of $Y_{10}I_{13}C_2$ is in itself remarkable in providing the first examples of several features: mixed chains, an empty iodide chain, and metallic and semiconducting chains simultaneously. This particular arrangement is particularly novel as it "captures" the Y_4I_6 fragment with a commensurate mode of the

(24) Lokken, D. A.; Corbett, J. D. *Inorg. Chem.* **1973**, *12*, 536.
(25) Simon, A.; Holzer, N.; Mattausch, Hj. *Z. Anorg. Allg. Chem.* **1979**, *456*, 207.
(26) Adolphson, D. G.; Corbett, J. D. *Inorg. Chem.* **1976**, *15*, 1820.
(27) Bauhofer, W.; Simon, A. *Z. Naturforsch.* **1982**, *37A*, 568.
(28) Bauhofer, W.; Simon, A.; Griffith, A. *Z. Naturforsch.* **1982**, *37A*, 564.
(29) Bullett, D. W. *Inorg. Chem.* **1980**, *19*, 1780.
(30) Ziebarth, R. P.; Corbett, J. D. *J. Am. Chem. Soc.* **1989**, *111*, 3272.

vital intercluster bridging that is no longer possible in the binary R_4X_6 structure.

Acknowledgment. We thank Lee Daniels and Harvey Burkholder for helpful discussions and Robert A. Jacobson for the provision of some of the diffraction and software facilities. Part of this research was supported by the National Science Foundation—Solid State Chemistry—under Grants DMR-8318616 and DMR-8902954 and was carried out in the facilities of the Ames Laboratory—DOE. Partial support was also provided by the donors to the Petroleum Research Fund, administered by the American Chemical Society.

Supplementary Material Available: Tables of detailed data collection and refinement information and thermal displacement parameters for $Y_{10}I_{13}C_2$ (2 pages); observed and calculated structure factors for $Y_{10}I_{13}C_2$ (5 pages). Ordering information is given on any current masthead page.

Contribution from the Department of Chemistry and Biochemistry, University of Notre Dame, Notre Dame, Indiana 46556, and Department of Chemistry, Purdue University, West Lafayette, Indiana 47907

Synthesis of Cobalt–Tungsten Clusters with Tetrahedral Metallic Cores Using the Mixed-Metal Complex $CoW(CO)_7(\eta^5\text{-}C_5H_4Me)$ (Co–W) as a Cluster Building Block. X-ray Diffraction Study of the Sterically Crowded Tetrahedral Cluster $CoW_3(CO)_9(\eta^5\text{-}C_5H_4Me)_3$

Michael J. Chetcuti,*[†] John C. Gordon,[†] and Phillip E. Fanwick[‡]

Received November 14, 1989

Cobalt–tungsten clusters with tetrahedral Co_xW_{4-x} (x = 1–3) cores are formed when $[W(CO)_2(\eta^5\text{-}C_5H_4Me)]_2$ (W≡W) or $Co_2(CO)_8$ is treated with $(OC)_4Co\text{-}W(CO)_3(\eta^5\text{-}C_5H_4Me)$ (**1b**). **1b** reacts with $[W(CO)_2(\eta^5\text{-}C_5H_4Me)]_2$ affording clusters $Co_2W_2(\mu_2\text{-}CO)_3(CO)_7(\eta^5\text{-}C_5H_4Me)_2$ (**2b**) and $CoW_3(CO)_9(\eta^5\text{-}C_5H_4Me)_3$ (**3b**), whose structure was established by a single-crystal X-ray diffraction study. **3b** crystallizes in the monoclinic space group $C2/c$ (No. 15) with a = 30.740 (6) Å, b = 9.706 (1) Å, c = 18.729 (4) Å, β = 91.78 (1)°, V = 5585 (3) Å^3, and Z = 8; refinement converged at R = 0.032, R_w = 0.041. The molecule contains a slightly flattened CoW_3 tetrahedral metallic core and has a pseudo-C_3 axis. The cobalt atom is ligated to three carbonyl ligands, while each tungsten atom is linked to a η^5-methylcyclopentadienyl ligand and two carbonyl groups. **3b** exhibits dynamic behavior that involves carbonyl ligand exchange; the ^{13}C NMR resonances of the $\eta^5\text{-}C_5H_4Me$ group are also temperature dependent. This cluster has C_3 symmetry in solution at −80 °C on the ^{13}C NMR time scale, but at or above 20 °C the effective symmetry is C_{3v}. The heterotrimetallic cluster $CoMoW_2(CO)_9(\eta^5\text{-}C_5H_4Me)_3$ (**3'**) was prepared by reacting **1b** with $[W(CO)_2(\eta^5\text{-}C_5H_4Me)]_2$ (W≡W), and its ^{13}C NMR spectrum was also studied. The cluster $Co_3W(\mu_2\text{-}CO)_3(CO)_8(\eta^5\text{-}H_4Me)$ (**5b**) and an unidentified cobalt species formed when **1a** was treated with $Co_2(CO)_8$. The pyrolysis of **1b** and the reaction of $Co_2(CO)_8$ with $[W(CO)_2(\eta^5\text{-}C_5H_4Me)]_2$ (W≡W) are described.

Introduction

A multitude of mixed-metal clusters have been characterized, and new species continue to be reported. Many heterometallic tetrahedral clusters containing combinations of the ubiquitous isolobal fragments $Ni(\eta^5\text{-}C_5H_5)$, $Co(CO)_3$, $M(CO)_2(\eta^5\text{-}C_5H_5)$ (M = Mo, W), and RC are known,[1] but others remain elusive owing to the lack of readily available syntheses. Our current research involves reactions of heterobimetallic compounds;[2] our serendipitous preparation of Ni_3W and Ni_3Mo clusters from nickel–molybdenum and nickel–tungsten dinuclear species[3] led us to explore whether other mixed-metal complexes had potential as better routes to known clusters or as building blocks to new compounds. The dimetallatetrahedrane species $(OC)_4CO(\mu\text{-}\eta^2,\eta^2\text{-}MeC_2R)W(CO)_2(\eta^5\text{-}C_5H_5)$ (R = Me, Ph) and related cobalt–molybdenum compounds are known.[4] The isolobal analogy suggests that tetrahedral clusters with Co_xW_{4-x} (x = 1–3) metallic cores should be accessible. Here we describe reactions of $(OC)_4C\text{-}W(CO)_3(\eta^5\text{-}C_5H_4Me)$ (**1b**) with $[W(CO)_2(\eta^5\text{-}C_5H_4Me)]_2$ (W≡W) and $Co_2(CO)_8$ and the thermolysis of **1b**, all of which lead to mixed-metal clusters. The X-ray structure and VT ^{13}C NMR behavior of $CoW_3(CO)_9(\eta^5\text{-}C_5H_4Me)_3$, a cluster that results from the reaction of **1b** with $[W(CO)_2(\eta^5\text{-}C_5H_4Me)]_2$ (W≡W), are presented, and a few reactions of the analogous cobalt–molybdenum complex $(OC)_4Co\text{-}W(CO)_3(\eta^5\text{-}C_5H_4Me)$ (**1a**) with some of these reagents are also discussed. We use **1a** and **1b** rather than their previously reported cyclopentadienyl analogues,[5] as the multiplet patterns exhibited by C_5H_4Me nuclei allow additional symmetry information to be gleaned from ^1H and ^{13}C NMR spectra.

Results and Discussion

(a) Reaction of $(OC)_4Co\text{-}W(CO)_3(\eta^5\text{-}C_5H_4Me)$ (1b) with $[W(CO)_2(\eta^5\text{-}C_5H_4Me)]_2$ (W≡W). (i) Reaction Products. $[W(CO)_2(\eta^5\text{-}C_5H_4Me)]_2$ (W≡W) and **1b** react to form three compounds that were separated chromatographically. The dimeric tungsten species $[W(CO)_3(\eta^5\text{-}C_5H_4Me)]_2$ was identified by IR spectroscopy. Two other products (**2b** and **3b**) were crystallized from hexanes. The dark colors of these complexes (**2b** is dark green; **3b** is purple) and their low solubilities and chromatographic mobilities are characteristic of metal clusters, and this was confirmed by spectroscopic analyses.

No meaningful MS data could be obtained for **2b** or **3b**: the clusters are involatile at low probe temperatures and decompose

[†] University of Notre Dame.
[‡] Purdue University.

(1) (a) Stone, F. G. A. *Angew. Chem., Int. Ed. Engl.* **1984**, *23*, 89. (b) Chetcuti, M. J.; Chetcuti, P. A. M.; Jeffery, J. C.; Mills, R. M.; Mitrprachachon, P.; Pickering, S. J.; Stone, F. G. A.; Woodward, P. *J. Chem. Soc., Dalton Trans.* **1982**, 699. (c) Beurich, H. Vahrenkamp, H. *Angew. Chem., Int. Ed. Engl.* **1981**, *20*, 98. (d) Mlekuz, M.; Bougeard, P.; Sayer, B. G.; Faggiani, R.; Lock, C. J. L.; McGlinchey, M. J.; Jaouen, G. *Organometallics* **1985**, *4*, 2046. (e) Jensen, S.; Robinson, B. H.; Simpson, J. *J. Chem. Soc., Chem. Commun.* **1983**, 1081.
(2) (a) Chetcuti, M. J.; Green, K. A. *Organometallics* **1988**, *7*, 2450. (b) Chetcuti, M. J.; Fanwick, P. E.; Grant, B. E. *J. Am. Chem. Soc.* **1989**, *111*, 2743. (c) Chetcuti, M. J.; Fanwick, P. E.; Gordon, J. C.; Green, K. A.; Morgenstern, D. *Organometallics* **1989**, *8*, 1790. (d) Chetcuti, M. J.; McDonald, S. R.; Rath, N. P. *Organometallics* **1989**, *8*, 2077.
(3) Chetcuti, M. J.; Huffman, J. C.; McDonald, S. R. *Inorg. Chem.* **1989**, *28*, 238.
(4) Wido, T. M.; Young, G. H.; Wojcicki, A.; Calligaris, M.; Nardin, G. *Organometallics* **1988**, *7*, 452.
(5) Abrahamson, H. B.; Wrighton, M. S. *Inorg. Chem.* **1978**, *17*, 1003.

0020-1669/90/1329-3781$02.50/0